ELSEVIER

28 October 1996

PHYSICS LETTERS A

Physics Letters A 222 (1996) 141–147

A long-period conical pendulum for vibration isolation

J. Winterflood, D.G. Blair [1]

Department of Physics, University of Western Australia, Crawley, Australia

Received 23 October 1995; revised manuscript received 14 June 1996; accepted for publication 30 July 1996
Communicated by P.R. Holland

Abstract

A practical design for a long-period conical pendulum based on the Scott–Russel linkage is presented together with proof-of-concept measurements on a simple prototype showing good stability for periods in excess of 20 seconds. The design is intended as a vibration isolation component for gravitational wave detection.

1. Introduction

The sensitivity of terrestrial gravitational wave detectors is limited at low frequencies by the degree of seismic isolation obtainable. Efforts to improve this isolation have resulted in several proposed very-low frequency passive isolators. The two most promising devices, the folded pendulum [1] and the X-pendulum [2], suspend a test mass from a linkage arrangement such that its motion mimics that of a very long simple pendulum. Unfortunately both devices are most easily implemented as one-dimensional isolators. Two one-dimensional isolator stages may be cascaded to obtain isolation in both horizontal directions (x and y) but there are significant constructional problems with this approach. The main problems arise from the requirement that both stages must be rigidly aligned with gravity within their operating plane and the rigidity required increases as the square of the pendulum period. Also the first cascaded stage (say x) provides no isolation in the y direction, which means that the y stage must be very well balanced and orthogonally aligned to the x stage to avoid coupling to the y motion which will bypass the first stage.

The design presented here avoids these problems by using a linkage arrangement which mimics the motion of a very long *conical* pendulum achieving x–y isolation in a single stage. It is based on the Scott–Russel linkage [3] which is then generalised to cylindrical symmetry to provide the required large radius spherical motion.

2. Geometry of motion

Fig. 1 shows a schematic of the essential linkage geometry. It consists of a normal pendulum of length r joined near the mid-point of a beam of length $a+b$. The normal pendulum is under tension and supports the entire weight of the structure and suspended mass. The top section of the beam supports the suspended mass under compression (and bending). The lower end of the beam is merely con-

[1] E-mail: dgb@earwax.pd.uwa.edu.au.

PII S0375-9601(96)00619-6

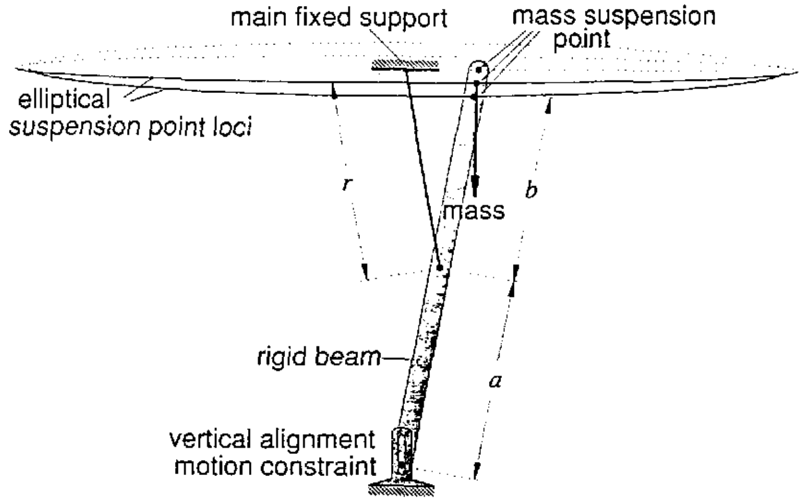

Fig. 1. Geometrical schematic. Pendulum r is under tension and carries the weight of the structure. The lower end of the rigid beam is constrained to move in a vertical line and a is typically made equal to r. The suspension point b may be chosen to give straight-line or large-radius curved motion.

strained to move in a vertical line directly under the main support.

If length a is made equal to r then the upper section of the beam b may be considered as an inverted pendulum which is constrained to follow the same angle of deflection as the normal pendulum a. If b is also equal to r then the effect of the normal and inverted pendulums cancel and the suspension point follows a straight horizontal line. If a slightly lower suspension point is chosen, then the suspension point follows an exact elliptical path as shown which may in principle be set to any large radius for small displacements. The linkage may be given cylindrical symmetry to produce spherical motion. There are some spatial conflicts, but these are readily overcome with a little ingenuity.

Letting $A = a/r$ and $B = (a+b)/a$, the full equation of motion of the suspension point in a single plane $(x–z)$ with the fixed support at $(x=0,\ z=0)$ is

$$z(B-1)\sqrt{A^2r^2 - x^2/B^2} - \sqrt{r^2 - x^2/B^2}. \qquad (1)$$

If $a = r$ $(A = 1)$ then this equation may be simplified to

$$\frac{x^2}{B^2r^2} + \frac{z^2}{(B-2)^2r^2} = 1, \qquad (2)$$

which is the equation of an ellipse centred about the fixed support with turning points at $\pm Br$ horizontally and $\pm(B-2)r$ vertically.

For this application $a \approx r$ and $b \approx r$, so we may replace $a \to r - a'$ and $b \to r - b'$ in Eq. (1) where a' and b' now represent the difference in length of a and b from the straight-line arrangement of $a = b = r$. The restoring force produced by gravity g acting on a mass m suspended by this geometry is then given by

$$F = -mg\left(\frac{b'-2a'}{4r^2}x + \frac{b'-4a'}{32r^4}x^3 + \dots\right). \qquad (3)$$

By choosing the relationship $a' = b'/4$, the x^3 term vanishes and the motion becomes closer to parabolic rather than elliptical. However, this improvement is probably insignificant for the small displacements expected from seismic disturbances. Assuming the simplest arrangement $a = r$ then the resonant frequency in Hz is given by

$$f = \frac{\sqrt{gb'}}{4\pi r}. \qquad (4)$$

For a beam length of 1 m ($r = 0.5$ m) and a resonant period of 60 s, the suspension point is ~ 1 mm below the straight-line or quasi-stable point ($b' = 1.1$ mm).

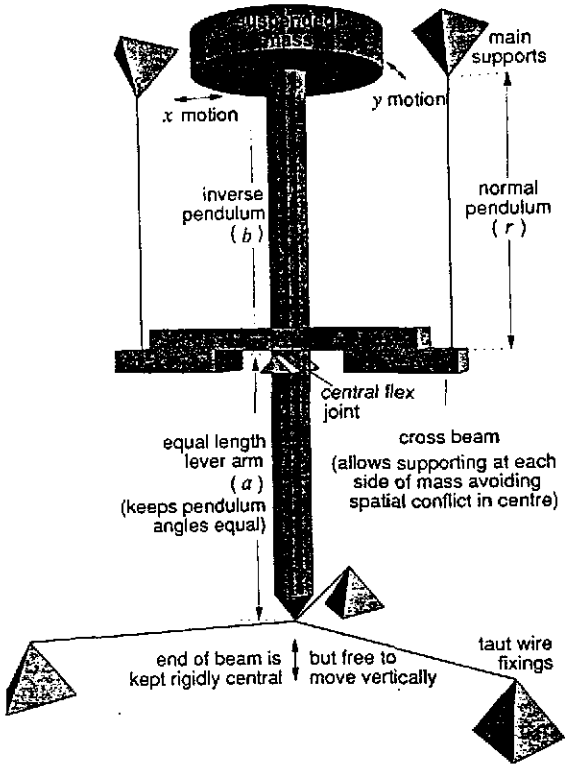

Fig. 2. Prototype arrangement. The vertical wires carry the entire weight of the structure as a normal pendulum. The vertical beam was a threaded rod and the suspended mass a threaded disk for ease of height adjustment.

3. Measurements

A simple prototype as shown in Fig. 2 was constructed in order to prove the concept. The beam was actually a threaded rod approx. 500 mm long and the suspended mass was a threaded disc. This allowed the "suspension point" to be adjusted up and down easily. With the cross beam arrangement the pendulum lengths (r) in the sideways direction (x) and the forward-and-back direction (y) can be independently set. Length r_y is the average length of the support wires at each side, while length r_x may be different if the central flex joint is not arranged to be at exactly the same level as the lower end of the support wires. This is the reason for the dog-leg shaped cross beam. These lengths were about 1 mm different for the measurements taken and this shows up as different resonant frequencies for the x and y directions. The beam was rather thin (6 mm threaded rod) for the mass supported but this allowed the effect of beam flexibility to be explored. The mass was initially adjusted for maximum repeatable period and then moved down in small amounts measuring the resonant frequency for each direction at each position. The process was repeated with a much heavier mass for comparison and the results are shown in Fig. 3. The amplitude of the motion used was between 1 cm and 3 cm p-p.

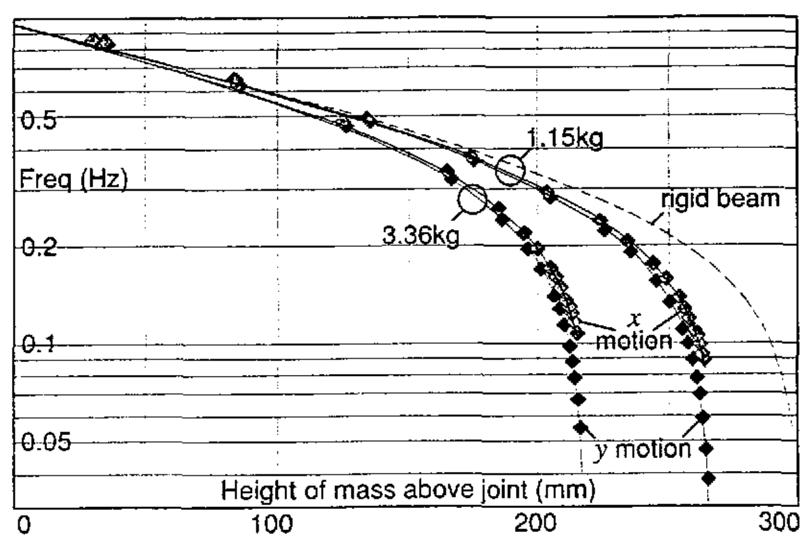

Fig. 3. Plots of frequency versus height. Points show the frequency of two different masses in the x and y directions as a function of mass height. The lines are curves fitted from theory.

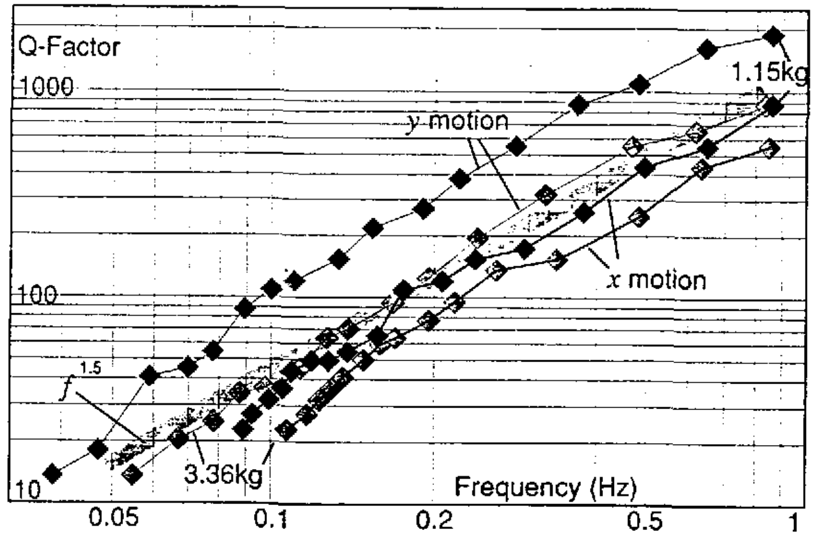

Fig. 4. Plots of Q-factor versus frequency. Points show the Q-factor of each resonance as a function of frequency. The joining lines are only to aid the eye in grouping the points. The slopes show a close $f^{1.5}$ dependence.

The large difference in the frequency versus height curves for the two different masses was due to the flexibility of the beam. The difference between the x and y directions was partly due to the 1 mm joint offset mentioned and partly due to differing beam flexibility from the flex joint construction in the centre of the beam.

The Q-factor of each resonance was measured by counting the number of cycles required for a ratio drop in amplitude. These results are shown in Fig. 4. The poor Q-factor in the x direction by comparison with the y direction was due to the central flex joint which is only active for x motion. This joint was rather lossy – the wire just passing around a slight V slot (not visible in the drawing) whereas the main supporting wires had crimped aluminium joints. The difference in Q-factor between the heavy and light masses varies oppositely to what might be expected, but this is not surprising in the light of other experimenters' experience and is discussed below.

4. Resonant frequency

Ideally the only force acting on the mass would be the restoring force due to the geometry of the motion and its alignment with gravity. Deriving this from Eq. (1) with $a \approx r$ and to first order in x gives a spring constant ($k = -\mathrm{d}F/\mathrm{d}x$) of

$$k_{\mathrm{geom}} = mg\frac{a(ab + ar - 2br)}{(a+b)^2 r^2}. \tag{5}$$

The effect of most of the non-ideal aspects of a physical implementation (beam, frame, and mounting flexibility, taut wire stretch, etc.) is to produce an anti-restoring force proportional to the offset. It may be modelled as a spring constant with opposite polarity to that of the restoring force. The dominant component of this spring constant for this prototype was the beam flexibility resulting from its area moment of inertia I_A and Young's modulus E_Y. Its value is given by

$$k_{\mathrm{bend}} = -(mg)^2\frac{2b^2}{3(a+b)E_Y I_A}. \tag{6}$$

The effect of the finite stiffness of the flexible joints may be modelled as a positive spring constant k_{flex} which simply adds to the other two. For an inertial mass of m_i the resonant frequency of this combination of spring constants is then

$$f = \frac{1}{2\pi}\sqrt{\frac{k_{\mathrm{geom}} + k_{\mathrm{bend}} + k_{\mathrm{flex}}}{m_i}}. \tag{7}$$

The extra mass of the beam m_b and the cross-member m_c need to be added to the value of the suspended mass m_s before appearing as m in Eqs. (5) and (6). The effective height b in these equations is also less than the measured height b_m,

$$m = m_s + m_b + m_c, \tag{8}$$

$$b = b_m m_s / (m_s + m_b + m_c). \tag{9}$$

The effective inertial mass is not simply the gravitational mass m because although the centre of mass may move in an almost straight line, the beam and suspended mass rotate significantly. The effective inertial mass of an object with moment of inertia I which is constrained to rotate as it moves, about a radius of length $(a+b)$ is

$$m_{eff} = m + I/(a+b)^2. \tag{10}$$

Applying this to both the suspended mass (a flat disc of radius r_m) and the vertical beam (a long thin rod) gives an effective inertial mass m_i for Eq. (7) of

$$m_i = m_s\left(1 + \frac{r_m}{4(a+b)^2}\right) + \tfrac{4}{3}m_b + m_c. \tag{11}$$

This mathematical model is sufficient to fit the measured points quite well as shown in Fig. 3. Most parameters were known but some which were not easy to determine exactly were obtained by optimising the curve fit. The known parameters were

$r_y = 258$ mm, $r_x = 257$ mm,

$a_y = 260$ mm, $a_x = 261$ mm,

$m_{s1} = 1.15$ kg, $m_{s2} = 3.36$ kg,

$m_b = 94$ g, $m_c = 34$ g,

$r_{s1} = 9$ cm, $r_{s2} = 12$ cm.

The fitted parameters were

b_m to b scale coincidence offset for m_{s1}, m_{s2}, x, y,

$E_Y I_A(x) = 8.67$ N m^2

(calc. 6.3 for 5 mm, 13 for 6 mm),

$E_Y I_A(y)/E_Y I_A(x)$ ratio = 1.04,

$k_{flex} = 0.25$ N/m.

5. Q-Factor

The Q-factor measurements were more approximate but show some interesting details. The overall trend as indicated by the faint wide band is that the Q-factor varies with frequency to a power of approximately 1.5. We shall consider some models to explain this.

If the damping force was proportional to velocity (viscous) then we would have the classical equation for damped harmonic motion $m\ddot{x} = -kx - d\dot{x}$ for a mass m with restoring force factor k and dissipation factor d. Solving this gives a resonant frequency ω_0 of $(k/m)^{1/2}$ with a Q-factor of $(km)^{1/2}/d$. Equating k in the two equations as the parameter being varied by adjusting the height of the mass gives $Q = \omega_0 m/d$ indicating that this model predicts that the Q-factor would vary proportionally to resonant frequency and mass.

It has been found that there are damping mechanisms which are frequency independent (i.e. no $\dot{x}$ term) over many decades of frequency. The effect is often termed structural damping and has been the subject of considerable investigation recently [4,5]. Two main areas have been noted [5], one being the intrinsic loss of the material and the other being stick and slip losses at clamped joints. The first is independent of amplitude whereas the second is strongly amplitude dependent. The damping effect is usually modelled in the frequency domain by a restoring force factor which has a small complex component. This gives an equation of motion of the form $m\ddot{x} = -k(1+i\phi)x$ where ϕ is termed the loss angle and is a characteristic of the stressed material. Solving this gives a resonant frequency of $(k/m)^{1/2}$ with a Q-factor of $1/\phi$. In our case only the material spring constants (i.e. k_{bend} and k_{flex}) which we will collectively call k_m can have this loss component ϕ_m. The main adjustable geometrical spring constant k_{geom} which we will now call k_g is due to gravity which is conservative. Substituting the sum of k_m (with ϕ_m) and k_g into the equation of motion and solving gives $\omega_0^2 = (k_g + k_m)/m$ and $Q = 1/\phi_m \times (k_g + k_m)/k_m$. Equating the $(k_g + k_m)$ terms gives $Q = \omega_0^2 m / k_m \phi_m$. So from this model we would expect the Q-factor to vary as ω_0^2 provided k_m stays reasonably constant. The flexure component of k_m should not change with k_g adjustment and it is expected that this is the main contributor to the losses since the flexing is very localised with high stresses at joints whereas the beam bend is evenly distributed over a monolithic rod.

So it seems that there is a significant component of both viscous and structural damping present which gives the intermediate power relationship. There is also a distinct concave downward tendency and this suggests that structural damping becomes more dominant at the lower resonant frequencies and vice versa. We expect that air friction and turbulence become significant at the higher frequencies.

With these relationships indicating that the Q-factor should vary directly with the mass for either damping mechanism, it may seem odd that an almost inverse relationship was observed. However the experimenters in Ref. [5] showed that stick and slip losses in clamps are strongly amplitude and stress dependent (significant amplitude dependence was observed in our case) and this dominates any intrinsic material loss. This means that the loss angle ϕ_m can increase greatly with additional loading. Also they found that even carefully designed kinematic weight mountings produced significant losses which disappeared after screwing them down tightly. In our case the heavier mass was measured first and when the lighter mass was measured it was found to inconsistently produce high losses due to movement between it and the threaded rod. So a lock nut was added to prevent this – possibly resulting in a considerable improvement over the heavier mass which was not tightly clamped. We thank a referee for drawing our attention to Ref. [5].

6. A practical implementation

The linkage structure shown in Fig. 2 is not suitable for suspending further structures as the rigid beam gets in the way. If it were inverted and the pendulum wires made into rigid rods with torsionally rigid flex hinges then it would become more suitable. However the entire height of this low-frequency stage would then add to the height of any structure suspended below it which could be excessive. A better approach seems to be to provide three linkages, each of which support one corner of a triangular platform which then provides a level surface as well as being horizontally isolated to low frequencies. In this way the height of the low-frequency isolating stage can be made to overlap with the height of any suspended structure, the overall height being greatly reduced.

Beam rigidity is a prime requirement with this design. Large diameter tubular section is most suitable and rather than weakening it with holes in the middle for a cross-beam, the main support pendulum wire can be made concentric within the tube. This also ensures that the x and y pendulum lengths are identical. Fig. 5 shows two such tubular beams in cross section with a platform suspended between them. The main support is at the top centre of the tube and the weight is taken by the thin central wire under tension. The lower end of the beam is connected by a flexible joint and a frame to the lower end of the other beams. This frame is constrained to only move vertically in some manner – taut wire guidance being simple and adequate. The upper end of the beam can move horizontally a few centimetres with the main support acting as a limit to this

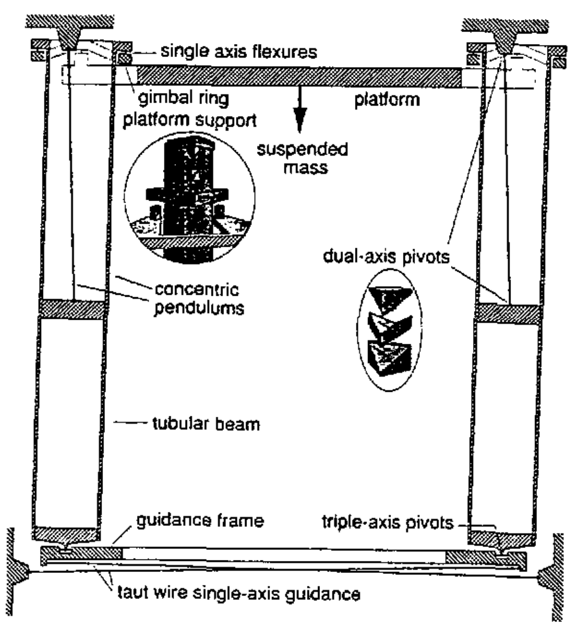

Fig. 5. Schematic of a practical implementation. Three linkages (only two shown) can support a triangular platform providing a level, horizontally isolated surface. Concentric pendulums ensure equal x and y performance.

motion. The triangular platform is not easily supported centrally by the beam as this space is used by the main support. However, a gimbal arrangement made with flexure pivots may be used to overcome this difficulty. An exploded diagram of a simple arrangement is shown as an inset together with a simple design for a dual axis flexible pivot. The flexures shown may be made from a monolithic block by spark erosion wire cutting. The lower flexible joints need to be able to cope with some twist about the vertical axis for the torsional motion which becomes possible with a platform supporting design. However these lower joints do not carry a significant load.

As with any vibration isolation system incorporating a rigid (i.e. massive) pendulum, care must be taken to suspend the isolated stage from the centre of percussion of the rigid pendulum. This is easily accomplished in this design by extending the beam tubes above the platform by an appropriate amount and adding some weight to their top ends. This has not been shown in the figure for the sake of simplicity.

7. Conclusion

From the measurements made it is evident that this Scott–Russel linkage performs as expected and can readily be generalised to simulate large-radius spherical motion. It is also evident that with some ingenuity it can be applied as a low-frequency horizontal isolation stage achieving x–y isolation in a single stage. We consider that the application of this concept to isolation for gravitational wave detection is worthy of further investigation.

References

[1] J. Liu, J. Winterflood and D.G. Blair, Rev. Sci. Instrum. 66 (1995) 3216.
[2] N. Kanda, M.A. Barton and K. Kuroda, Rev. Sci. Instrum. 65 (1994) 3780.
[3] J.S. Beggs, Mechanism (McGraw-Hill, New York, 1955).
[4] P.R. Saulson, R.T. Stebbins, F.D. Dumont and S.E. Mock, Rev. Sci. Instrum. 65 (1994) 182.
[5] T.J. Quinn, C.C. Speake, R.S. Davis and W. Tew, Phys. Lett. A 197 (1995) 197.